Modification to the Toroidal Rotation Velocity and Radial Electric Field by Pellet Injection in DIII-D

L.R. Baylor[1], P. Gohil[2], K.H. Burrell[2], T.C. Jernigan[1], W.A. Houlberg[1]

[1]*Oak Ridge National Laboratory, Oak Ridge, Tennessee, USA.*

[2]*General Atomics, San Diego, California, USA*

Introduction

The ability to modify and control the radial electric field and its radial derivative can lead to direct control of radial transport of plasma in a toroidal device. In the DIII-D tokamak, the injection of deuterium pellets is being investigated as a means of controlling the toroidal rotation velocity and the radial electric field, E_r. Solid deuterium cylindrical pellets of 1.8mm and 2.7mm diameter have been injected into single null diverted plasmas at 1.0 MA and 2.1T. Plasmas with either upper null or lower null diverted configurations were studied. The pellets have been injected from a number of locations including radial injection from the plasma outer midplane, vertically inside the magnetic axis, and from two locations on the inner wall. The penetration of the pellets is as deep as the axis for inner wall injection and to ρ=0.4 with radial outside midplane and vertical injection. The pellets significantly perturb the electron density profiles and initial results indicate a decrease in the toroidal rotation velocity such that toroidal angular momentum is conserved. From a radial force balance analysis it is seen that the injected pellets can significantly affect the radial profile of E_r.

Pellet Perturbations

Deuterium pellet injection from inner wall, vertical, and outer midplane launch locations has been employed on the DIII-D tokamak to investigate density control and transport barrier physics. The available injection locations are shown in a poloidal cross section in Fig. 1. Pellets injected from the outer midplane (low field side) show a large discrepancy in the mass deposition profile and fueling efficiency from pellet ablation theory, while the penetration depth compares favorably with theory [1]. An apparent outward displacement of the deposited pellet mass is observed and hypothesized to occur from ∇B and curvature induced drift effects [1,2,3]. Injection of pellets from the inner wall and a vertical port inside the magnetic axis using curved guide tubes has been employed on DIII-D to investigate these effects. The results show pellet mass deposition inside the expected penetration radius, suggesting that a drift of the pellet ablatant occurs in the major radius direction during the ablation process [4]. An example of this deep density deposition for a vertically injected pellet into a neutral beam heated H-mode plasma is shown in Fig. 2. Since the pellet mass undergoes a rapid major radius drift it is important to investigate whether the pellet density perturbation conserves angular momentum in the plasma after the deposition process. The determination of the plasma angular momentum before and just after pellet injection is thus an important part of this study.

This new capability to inject pellets from the inner wall is being used to compare the effect of pellets from different injection locations and sizes on the plasma toroidal rotation and on the E_r profile. Further analysis is underway to determine the subsequent changes in transport following modification to the E_r profile. Experiments are carried out with both co- and counter neutral beam injection. Also, a new capability to produce shattered pellets by employing a carefully bent guide tube has been developed and is used to create localized density perturbations at the plasma edge. These pellet perturbations are used to investigate whether edge-localized deuterium pellet deposition can modify ExB shear and lower the H-mode power threshold. The shattered pellets are also used in H-mode plasmas to trigger edge localized modes (ELMs) in order to extend the high performance phase of ELM-free plasmas.

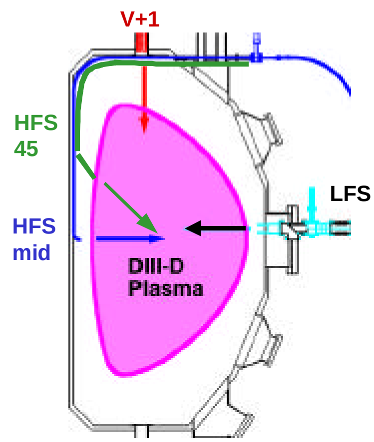

Fig. 1: The pellet injection locations on DIII-D shown in a poloidal cross section.

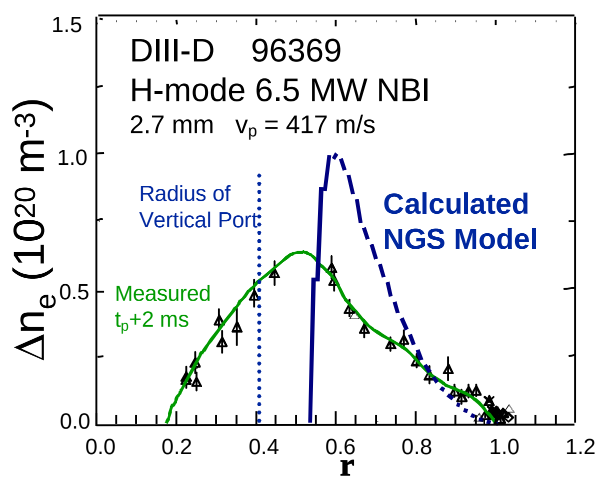

Fig. 2: The resulting density deposition profile from a 2.7mm deuterium pellet injected from the vertical injection port. The calculated deposition using the NGS model is shown for comparison.

Analysis Method

The diagnostic and analysis method used to determine the plasma angular momentum and radial electric field profiles [5] is shown schematically in Fig. 3. The measured profiles of electron density from Thomson scattering and carbon density from charge exchange recombination spectroscopy (CER) are used to determine the deuterium density profiles using Eqn. 1, which assumes that carbon is the dominant impurity.

$$n_D(r) = n_e(r) - 6n_C(r) \tag{1}$$

In this equation n refers to the density and the subscript D is the deuterium, e the electrons, and C the carbon.

The radial electric field is determined from the radial force balance [6] for the carbon species as given in Eqn. 2

$$E_r(r) = \frac{\nabla P_C(r)}{Z_C e n_C(r)} + v_{jC} B_q - v_{qC} B_j \tag{2}$$

where is the pressure, v_{jC} and v_{qC} are the toroidal and poloidal velocities, and the C subscript refers to the carbon species. The toroidal and poloidal magnetic fields (B_j , B_q) are obtained from the magnetic equilibrium calculation in the EFIT code [7]. The deuterium rotation velocity is not directly measured and must be determined from the radial electric field, which is of course the same for all species and is written for the deuterium species in Eqn. 3.

$$E_r(r) = \frac{\nabla P_D(r)}{Z_D e n_D(r)} + v_{jD} B_q - v_{qD} B_j \tag{3}$$

The poloidal velocity component of Eqn. 3, v_{qD}, is determined by assuming that it is given by the neoclassical value calculated in the NCLASS routines in the FORCEBAL code [8] from the measured carbon rotation data. This is believed to be a reasonable approximation, since the measured carbon poloidal velocity component is small and this term has a small effect in the radial force balance. The angular momentum of the deuterium species is then determined in Eqn. 4 by multiplying the deuterium density by the deuterium toroidal angular speed that is determined from Eqn. 3.

$$L_D(r) = n_D(r)\, \Omega_D(r) \tag{4}$$

The integration time of the CER measurement for these experiments was set to 2.5 ms in order to determine the pressure and change in the rotation velocity from the pellet accurately. The pellet ablation event typically lasts 0.3ms. The pellets were timed with respect to the Thomson scattering laser firing time to obtain the electron profiles within 2ms following the pellet injection event. Thus from these measurements it is possible to determine the pressure and rotation profiles approximately 2ms after the pellet event and, since the plasma is in steady state, the profile measurements 4ms before the pellet accurately represent the pre-pellet values.

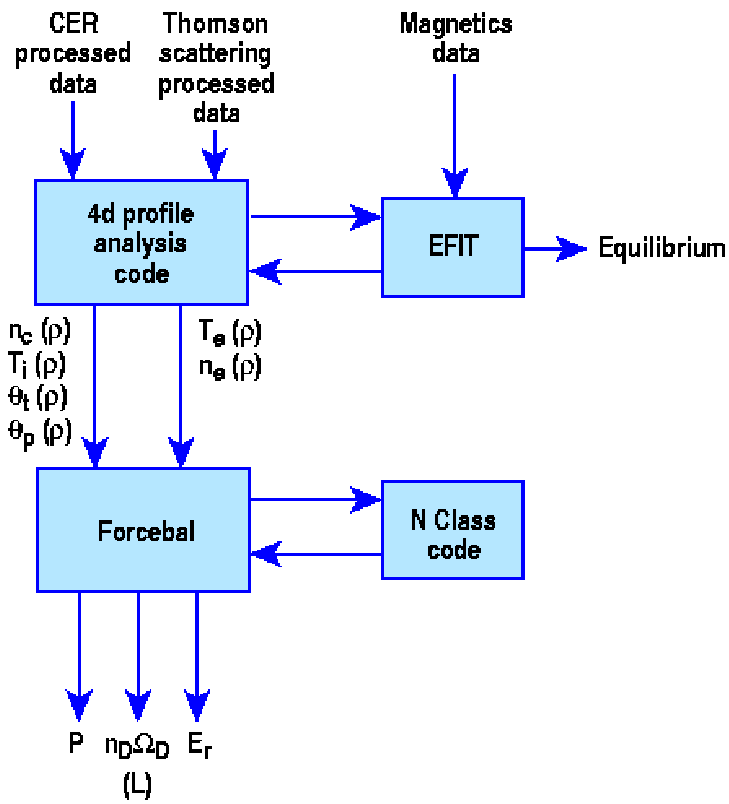

Fig.3: Block diagram of the analysis method used to determine the angular momentum, pressure, and radial electric field from the pellet perturbation on DIII-D.

Resulting Modifications to Rotation and Radial Electric Field Profiles

Measurements of the carbon rotation from the CER diagnostic show an immediate decrease in the toroidal rotation velocity. The radial electric field is determined from the carbon rotation data and is then used to calculate the deuterium toroidal rotation velocity, which also shows an immediate decrease. An example of the change in toroidal rotation velocity profile for the deep penetrating vertical 2.7mm pellet in Fig. 2 is shown in Fig. 4. The profiles inside of $\rho = 0.3$ are not shown because of incomplete coverage of the minor radius by the Thomson scattering diagnostic. By multiplying the deuterium rotation velocity by the density of deuterium we get a measure of the angular momentum. In Fig. 5 we show the angular momentum profile for the deuterium in the same vertical injection case shown in Fig. 4. In this example as in all others analyzed, the angular momentum is conserved within the measurement uncertainties in density and toroidal rotation velocity. This is true for different pellet sizes and pellet injection locations.

ρ

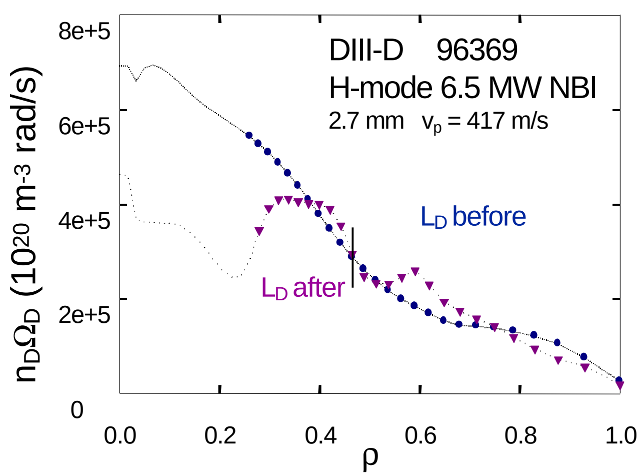

Fig. 5: The angular momentum of the main ion species before and 2ms after pellet injection showing that the angular momentum is conserved within the error bars of the measured quantities.

The pressure profiles before and immediately after injection are the same within the error bars for both the small 1.8-mm and large 2.7-mm pellets and does not depend on the injection location. Fig. 6 shows the pressure profile comparison for the 2.7-mm vertical pellet shown in the preceding figures. This means that all changes in the radial electric field are largely caused by the change in the plasma toroidal rotation caused by the pellet since this is usually the dominant term in Eqn. 3. With an accurate prediction of the pellet density perturbation it should then be possible to determine how a given pellet will change the radial electric field. Unfortunately due to the complicated major radius drift mentioned in the introduction, it is not yet possible to accurately model the pellet mass deposition, but efforts are under way to develop an accurate model of the deposition process [3].

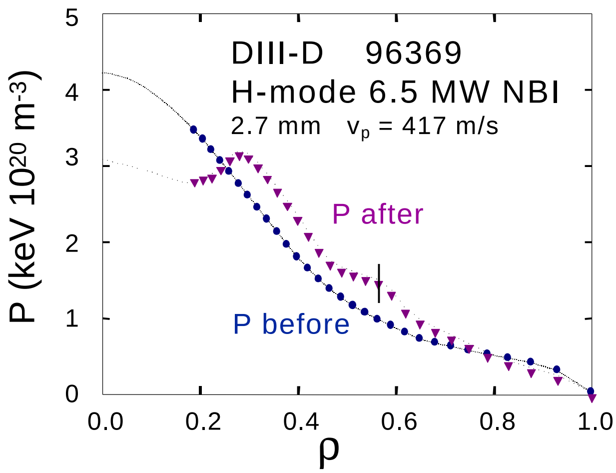

Fig. 6: Total plasma pressure before and just after injection of a 2.7 mm pellet from the vertical injection port. Within the error bars of the analysis, the pressure profile is conserved showing that the pellet deposition process is adiabatic.

In co-injected neutral beam heated plasmas the reduction in the toroidal rotation speed causes a decrease in the radial electric field as can be seen from Eqn. 3. This is shown for our vertical pellet injection case in Fig. 7. In this case because of the broad pellet mass deposition through most of the profile, the radial electric field decreases across the measured portion of the profile. For a shallower pellet the change in E_r is more localized where the rotation is changed. For counter neutral beam injection, which is accomplished on DIII-D by changing the direction of the plasma current, the change in rotation speed causes a local increase in E_r where the rotation is reduced. By utilizing this method it should in principle be possible to modify E_r in such a way to form an internal transport barrier either in the form of an edge barrier such as the L to H-mode transition or a core barrier as is seen in negative central shear discharges [6].

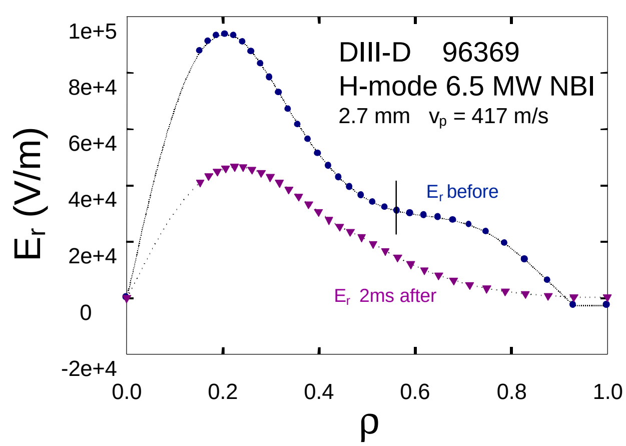

Fig. 7: The radial electric field before and 2ms after pellet injection as determined from the radial force balance.

The *ExB* shear damping rate [6] is the rate shear stabilization for flute-like modes and is given by Eqn. 5

$$w_{ExB} = \frac{(RB_q)^2}{B}\left(\frac{\partial}{\partial y}\right)\frac{E_r}{RB_q} \tag{5}$$

This rate is calculated for our vertical injection case and is shown in Fig. 8 to decrease across most of the profile. The sign of w_{ExB} is not relevant in the various theories for shear stabilization. What is apparent is that the shear in $\frac{\dot{}}{RB_q}$ has the most significant effect on the stabilization of turbulence and is the quantity that one wants to modify with the pellets to affect turbulence.

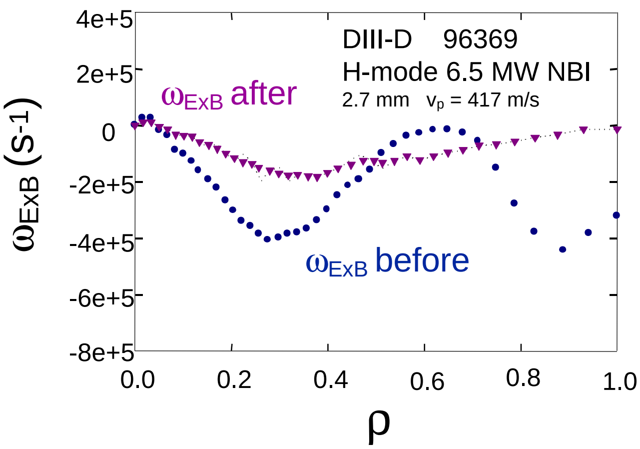

Fig. 8: The shear damping rate before and 2ms after vertical pellet injection. The rate decreases through most of the profile after injection in this case.

Summary

We have shown that deuterium pellets of the largest size used on DIII-D (2.7-mm diameter and length) are able to significantly reduce the toroidal rotation velocity of the plasma where the pellet mass is deposited such that the angular momentum is conserved. The pellet deposition process is adiabatic within our measurement accuracy and the pressure profile is not modified by the pellet despite the major radius drift of the pellet mass. The reduction in toroidal velocity leads to a local reduction in E_r through the radial force balance and hence a change in the shear damping rate. This capability to change E_r makes it desirable to use pellet injection to actively control the E_r profile at specific radii for the formation of transport barriers. New pellet injection tools on DIII-D using shattered pellets from the outside midplane and whole pellets with deep fueling from the inner wall are now being employed for such transport barrier formation experiments.

Acknowledgments

We gratefully acknowledge the assistance of the DIII-D operations group at General Atomics and the Plasma Fueling Group at Oak Ridge National Laboratory. This research was sponsored by the Office of Fusion Energy Science, U.S. Department of Energy, under contracts DE-AC05-96OR22464 and DE-AC03-99ER54463.

References

[1] L.R. Baylor, et al., Fusion Tech. **34** 425 (1998).
[2] P.T. Lang, et al., Phys. Rev. Lett. **79**, 1487 (1997).
[3] P.B. Parks, et al., EPS 1999 Conference Proceedings, (1999).
[4] L.R. Baylor, et al., EPS 1999 Conference Proceedings, (1999).
[5] P. Gohil, et al., Bull. Am. Phys. Soc., **43** (8) 1759 (1998).
[6] K.H. Burrell, Phys. Plasmas **4**, 4945 (1997).
[7] L. Lao, et al., Nucl. Fusion **30,** 1035 (1990).
[8] W.A. Houlberg, Phys. Plasmas **4**, 3230 (1997).